Observation of Dyakonov Surface Waves

Osamu Takayama,[1] Lucian Crasovan,[1] David Artigas,[1,2] and Lluis Torner[1,2]

[1]*ICFO-Institut de Ciencies Fotoniques, Mediterranean Technology Park, 08860 Castelldefels (Barcelona), Spain*

[2]*Department of Signal Theory and Communications, Universitat Politècnica de Catalunya, 08034 Barcelona, Spain*

(Received 12 June 2008; revised manuscript received 28 November 2008; published 28 January 2009)

We report the first experimental observation of Dyakonov surface waves existing at the interface of transparent anisotropic crystals. A Otto-Kretchmann configuration was used to excite the surface waves at the interface between a potassium titanyl phosphate biaxial crystal and an index-matching liquid fulfilling the conditions at which the waves exist. The signature of surface wave excitation was obtained by using enhanced polarization-conversion reflectance phenomena. We measured the cutoff propagation angles for different index-matching liquids, confirming the high sensitivity of the propagation conditions with the properties of the supporting interface.

DOI: 10.1103/PhysRevLett.102.043903 PACS numbers: 42.25.Lc, 41.20.Jb, 71.36.+c, 78.68.+m

Surface electromagnetic waves are a topic of outstanding current interest because of their unique properties and prospects of potential applications in different areas of science and technology. Surface waves are rare, as they are supported by only a few types of materials and geometries. One of the best known examples of surface waves are the so-called plasmon polaritons, which in the simplest cases exist at the boundary of a metal [1,2]. Surface plasmon polaritons show promise for diagnostic and therapeutic techniques [3], biosensing [4], microscopy [5], nano-optical-tweezing [6] or integrated optics [7]. They also play a key role in new phenomena as extraordinary transmission [8,9], enhanced Raman scattering [10,11], and are the basis of new light sources known as spasers [12,13]. Surface waves supported by the edge of photonic crystal structures [14,15] as well as by gyrotropic and chiral materials [16] are also known to exist.

A special type of surface wave was predicted by Dyakonov in 1988 [17]. Such waves exist under special conditions at the interface of transparent anisotropic materials, and thus they are lossless. These surface waves require that at least one of the two media is an anisotropic medium, either biaxial or positive uniaxial. In the case of the interface of a biaxial anisotropic medium with refractive indices n_x, n_y, and n_z, and an isotropic medium with refractive indices n_c, surface waves form only when the refractive indices fulfill the condition [18]

$$n_1 > n_c > n_2 > n_3, \tag{1}$$

where $n_1 = \max(n_x; n_y; n_z)$, $n_3 = \min(n_x; n_y; n_z)$, and n_2 is in between n_1 and n_3. For a positive uniaxial medium (1) reduces to $n_e > n_c > n_o$. When such a condition is fulfilled, hybrid surface waves containing both ordinary and extraordinary field components propagate within a narrow angular band $\Delta\theta$ relative to the crystal optical axis, around a central angle θ_c. The allowed propagation angles are referred to as the angular existence domain. Condition (1) does not commonly occur with natural materials, because the difference between the refractive indices of transparent anisotropic materials is typically tiny. Therefore, Dyakonov surface waves have been never observed experimentally to date. In this Letter we report the observation of their excitation in a sample based on a potassium titanyl phosphate (KTP) crystal.

Potassium titanyl phosphate is a biaxial crystal with relatively low refractive indices ($n_x = 1.7619$, $n_y = 1.7712$, and $n_z = 1.8648$ at $\lambda = 632.8$ nm [19]). This makes possible the use of nontoxic, noncorrosive, stable index-matching liquids as isotropic media, available with $n_c < 1.8$. In addition, polarization conversion phenomena [20] can be used as a new contrast mechanism to obtain signatures of the surface wave excitation.

Our experimental setup is based on a modified Otto-Kretchmann configuration (Fig. 1) where the index-matching liquid is placed between a ZnSe prism ($n_p = 2.589$) and the KTP crystal. An expanded beam of a He-Ne laser ($\lambda = 632.8$ nm) is focused at the interface through a polarizer, a $\lambda/2$ plate, a lens ($f = 150$ mm), and the ZnSe prism. The reflected beam is collected by an identical second lens, a polarizer, and directed to a CCD camera. In this way the intensity reflectance spectrum for a given

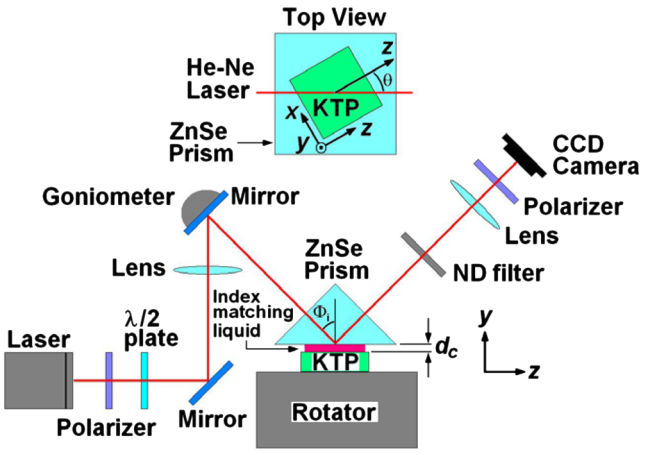

FIG. 1 (color online). Experimental setup.

input polarization (determined by the $\lambda/2$ plate) and output polarization (determined by the second polarizer) can be obtained. The diameter of the reflectance spectrum at the CCD sensor was about 0.15°. The internal angle of incidence φ is computer-controlled using a goniometer with a resolution $\Delta\varphi = 0.0001°$. The crystal orientation θ (propagation angle) with respect to the incident beam is controlled with a rotator with resolution $\Delta\theta = 0.01°$. We used a Y-cut KTP crystal. With this crystalline cut, the X axis and Z axis are parallel to the KTP-liquid interface, while the Y axis is perpendicular to the interface. The propagation angle θ is measured relative to the Z axis of the crystal, with $\theta = 0°$ corresponding to a crystal orientation with the Z axis contained in the plane of incidence. The two crystalline optical axes are contained in the plane of the interface at an angle $\theta_{oa} = \pm 19.18°$.

The prism-liquid-KTP structure described above was theoretically analyzed by using a transfer-matrix formalism [21]. In Fig. 2, we show the calculated reflectance spectra as a function of the internal angle of incidence within the prism φ and the propagation angle θ. The thickness of the index-matching liquid is $d = 4.75$ μm and $n_c = 1.7868$. The results are plotted for TE_{in}-TE_{out}, TM_{in}-TM_{out}, and TE_{in}-TM_{out} input-reflected output polarization (TE stands for transverse electric; TM for transverse magnetic). Note that the TE_{in}-TM_{out} and TM_{in}-TE_{out} configurations are equivalent. In these plots, the different critical angles corresponding to interfaces between the prism, and the index-matching liquid, φ_{cl}, the extraordinary wave, φ_{ce}, and the middle refractive index of the KTP crystal n_y, φ_{cy}, are shown as a reference.

In Figs. 2(a) and 2(b) areas with low reflection and dips are readily visible. The extended areas with low reflection are caused by transmission to the bulk crystal. Such areas are always located at incident angles below the critical angles φ_{ce} and φ_{cy}, depending on the incoming polarization. Between φ_{cl} and φ_{cy} clear reflection dips appear (as horizontal lines). These reflection dips are associated to half-leaky modes of the structure. Because of the biaxial anisotropy of the substrate, the radiation to the prism associated to the half-leaky modes results in a polarization conversion from TE- (TM-) incident light to TM- (TE-) reflected light. This conversion is clearly visible in Fig. 2(c), where reflection appears only at the position where there is a dip in Figs. 2(a) and 2(b). This polarization conversion near the critical angles depends on the actual refractive index and thickness of the index-matching liquid [20]. Our interest, however, lies in that the polarization conversion shown by Fig. 2(c) also appears for Dyakonov surface waves. Experimentally, observation of bright peaks in a black background using a CCD camera is easier than observation of dark peaks in a bright background. In addition, reflections which are not associated to modes supported by the structures do not result in polarization conversion, resulting in clearer images. Therefore, for practical purposes our experimental observation is based on polarization-conversion images, while reflection images maintaining the polarization are used for calibration purposes.

As shown by Fig. 2(b), the critical angle φ_{cy} for prism-KTP refractive index n_y appears as a sharp change in reflectivity, dividing a region with total reflection ($\varphi \geq \varphi_{cy}$) and a high transmission ($\varphi < \varphi_{cy}$). This allows calibrating the internal angle of incidence by observing TM_{in}-TM_{out} reflection images. This division line in the experiment showed a smoother transition resulting in an estimated experimental error of $\Delta\varphi_{err} = 0.02°$. Once the angle φ is calibrated, the thickness of the index-matching liquid can be calculated by comparing the position of

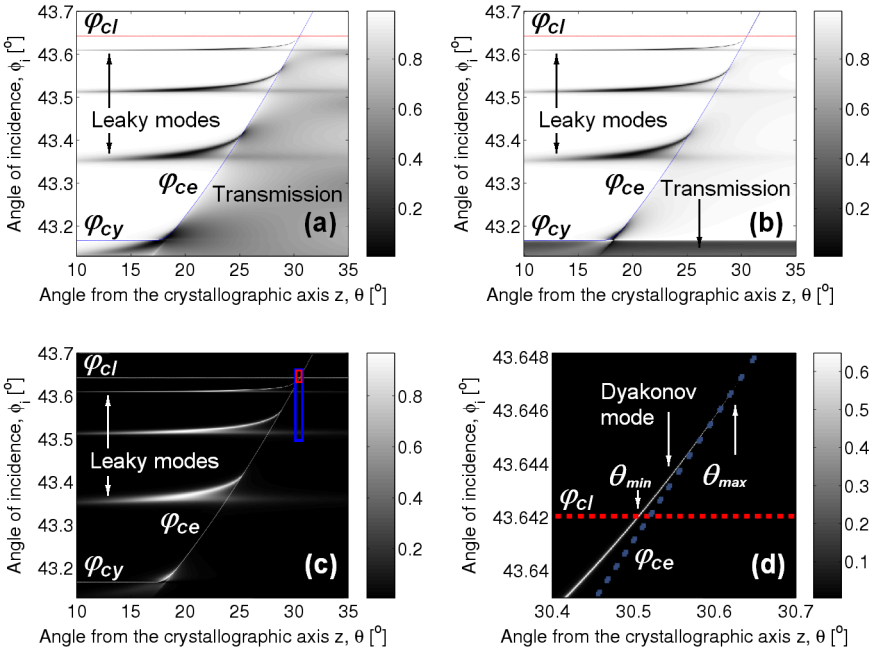

FIG. 2 (color online). Reflectance spectra for (a) TE_{in}-TE_{out}, (b) TM_{in}-TM_{out}, (c) TE_{in}-TM_{out}, input-output polarization. (d) Magnification of the small (red online) rectangle in (c). The lines labeled with φ_{cl}, φ_{cy}, and φ_{ce} are the critical angles between the prism and the index-matching liquid, the refractive index n_y, and the extraordinary refractive index of the KTP crystal, respectively. The large rectangle (blue online) shows the area corresponding to the experimental image in Fig. 3(a).

the different dips in the experimental TM_{in}-TM_{out} and TE_{in}-TM_{out} reflection images with the theoretical ones, resulting in thicknesses around $d = 4.7 \pm 0.3$ μm. Calibration of the θ angle was performed by taking into account that the reflectance spectrum is symmetric with respect to $\theta = 0°$. By measuring the reflectivity peaks at positive and negative angles, the actual position of the Z axis was obtained.

Among all the reflection peaks in Fig. 2(c), only those that have an incident angle above the critical angles φ_{cl} and φ_{ce} correspond to the surface waves [zoom in Fig. 2(d)]. The angular existence domain for the surface wave is determined by the cutoff for radiation into the index-matching liquid, giving the minimum allowed angle θ_{min}, and to the coupling to the continuous spectrum of the extraordinary wave in the KTP crystal, giving the maximum allowed angle θ_{max}. Below θ_{min} the peak in Fig. 2(d) has continuity. This is because the surface wave becomes a leaky mode (i.e., fields in the liquid are not evanescent anymore). Because of this continuity, this cutoff position cannot be experimentally determined with our experimental setup. In addition, the exact value of θ_{min} is affected by the actual thickness of the liquid reducing the experimental angular existence domain [22]. On the contrary, θ_{max} can be experimentally observed because the reflection peak disappears at this angle. In our calculations, this occurs when the peak intercepts the line corresponding to the critical angle φ_{ce}. The position of θ_{max} does not change with the thickness, and only depends on the refractive index of the index-matching liquid. In the case shown in Fig. 2, with a thickness of $d = 4.75$ μm and $n_c = 1.7868$, the calculated angular existence domain is around $\Delta\theta \sim 0.1°$, between $\theta_{min} = 30.5°$ and $\theta_{max} = 30.6°$.

We elucidated the cutoff angle θ_{max} at positive and negative angles as follows. First, the peaks located at the highest incident angles φ in the polarization-conversion reflectance spectrum are identified at propagation angles $\theta < \theta_{max}$. A typical image can be seen in Fig. 3(a), where two parallel lines can be observed. The weak line on the top corresponds to a Dyakonov surface wave, while the bottom line is a half-leaky mode, as justified below. From these images we only consider a central angular window of 0.05° corresponding to the beam width. The result is shown in Fig. 3(b). To enhance the peak brightness associated with the Dyakonov surface wave, the intensity image is integrated along the horizontal direction. Then, the top line appears as a clear secondary peak [Fig. 3(c)]. Because θ_{min} is not available, the top line in Fig. 3(b) may correspond to a surface wave or to its continuation as leaky mode. Thus, we increase the propagation angle θ until the partial disappearance of the top line is observed. In Fig. 3(d) this occurs at the middle of the image. Correspondingly, the peak in Fig. 3(e), shows a clear decrease. This indicates that the image corresponds to or is close to the cutoff. Note that the angular window of the image is smaller than the angular existence domain. Therefore, the top line corresponds to a Dyakonov surface wave. Finally, in Fig. 3(f) the top line associated to the surface waves is not observed while the corresponding peak in Fig. 3(g) has disappeared. Therefore, this image correspond to an angle $\theta > \theta_{max}$.

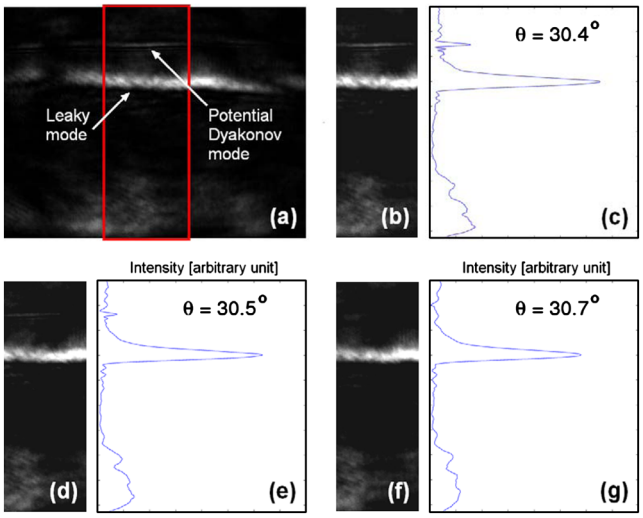

FIG. 3 (color online). Experimental observation for an M1.795 liquid (a) image obtained by CCD camera for $\theta = 30.4°$. Dimensions of the image in degrees: $0.21° \times 0.16°$ The rectangle indicates the portion of the image shown in (b) at $\theta = 30.4°$, (d) at $\theta = 30.5°$, and (f) at $\theta = 30.7°$. (c), (e), and (g) show the integrated intensity along the lateral direction for images (b), (d), and (f), respectively.

The images in Fig. 3 were obtained using an index-matching liquid (reference M1.795, Cargille Laboratories) with $n_c = 1.7868$ at the laboratory temperature of 23.0 °C and $\lambda = 632.8$ nm. With this refractive index, the calculated cutoff angle is $\theta_{max} = 30.63°$ with an angular existence domain $\Delta\theta = 0.13°$ (more than twice the angular window used for integration in Fig. 3). Using the calibration method described above, the image in Fig. 3(d) was obtained for $\theta = 30.5°$, showing a good agreement with theory. In some cases, we were not able to obtain a clear image as Fig. 3(d), where the peak can be observed disappearing, simultaneously in both positive and negative θ. This is the main source of error when determining the value of the cutoff angle θ_{max}.

We conducted >25 different experiments with five different index-matching liquids. In each series the temperature was monitored, and the actual values of the refractive index of the liquid were accordingly corrected. The results for the cutoff angle θ_{max} are shown in Fig. 4 together with the theoretical curve. The index-matching liquid used for the lower refractive index ($n_c = 1.7737$), which had a different chemical composition, resulted in images with least quality, and hence, a larger variation in θ_{max}. The remaining four liquids showed a good agreement between theoretical prediction and experimental results. Figure 4 illustrates a potential application of Dyakonov surface waves as highly sensitive refractive index sensors. Based on our experiments, a change in $\Delta n = 0.005$ causes a shift of the propagation angle θ by 3°, determining the sensi-

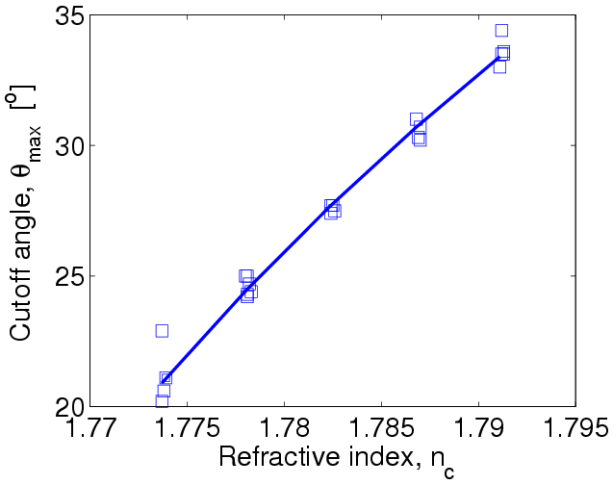

FIG. 4 (color online). Experimental cutoff angle θ_{max}. The results are presented for five different index-matching liquids (squares) together with the theoretical cutoff angle at $T = 23.0\,^{\circ}\mathrm{C}$ (solid line).

tivity in our setup. It is worth noting, however, that using the angle of incidence φ the peak associated with the surface wave is on the order of $\Delta\varphi = 0.0001^{\circ}$, which is 3 orders of magnitude narrower than the typical resonance dip in plasmons. Therefore, there is plenty of room to improve the resolution by using new materials and specific experimental setups.

Here Dyakonov surface waves were observed for an isotropic-biaxial birefringent material interface. However, possible configurations were such waves exist include also isotropic-uniaxial [17], uniaxial-uniaxial [23], and biaxial-biaxial interfaces [24], resulting in different propagation characteristics and experimental conditions (see Ref. [22] for a review). In addition, new effects and opportunities appear in combination with other material and geometrical properties, such as magnetic materials [25], thin films [26], nonlinear media [27], electro-optic effect [28], or voltage-controlled optical axis orientation in liquid crystals, to name a few. The use of photonic metamaterials, in particular, nanostructured materials exhibiting tunable form-birefringence, as anisotropic media is of particular interest [29]. In such a case, condition (1) can be met with a variety of parameter values, opening the door to engineering the propagation characteristic of the surface waves and their excitation conditions.

In conclusion, we reported the first observation of Dyakonov surface waves. We used a modified Otto-Kretchmann configuration to excite the surface waves in an index-matching liquid-KTP interface. Surface wave excitation was detected by imaging the polarization-conversion reflectance spectrum. Here we used a biaxial KTP transparent crystal and visible laser radiation, but it is worth stressing that similar phenomena occur in other physical settings, in particular, in nanostructured materials exhibiting form birefringence and in other bands of the electromagnetic spectrum.

This work was supported by the Government of Spain through Grants No. TEC2005-07815/MIC and No. FIS2006-10045. Support by Fundació Cellex Barcelona is also acknowledged.

[1] W. L. Barnes, A. Dereux, and T. W. Ebbesen, Nature (London) **424**, 824 (2003).
[2] H. Raether, *Surface Plasmons* (Springer-Verlag, Berlin, 1988); S. A. Maier, and H. A. Atwater, J. Appl. Phys. **98**, 011101 (2005).
[3] N. Kedei *et al.*, Cancer Res. **64**, 3243 (2004).
[4] D. A. Schultz, Curr. Opin. Biotechnol. **14**, 13 (2003).
[5] M. Specht *et al.*, Phys. Rev. Lett. **68**, 476 (1992).
[6] M. Righini *et al.*, Nature Phys. **3**, 477 (2007); M. Righini *et al.*, Phys. Rev. Lett. **100**, 186804 (2008); R. Quidant and C. Girard, Laser Photon. Rev. **2**, 47 (2008).
[7] H. Ditlbacher *et al.*, Appl. Phys. Lett. **81**, 1762 (2002).
[8] T. W. Ebbesen *et al.*, Nature (London) **391**, 667 (1998).
[9] L. Martín-Moreno *et al.*, Phys. Rev. Lett. **90**, 167401 (2003).
[10] K. Kneipp *et al.*, Phys. Rev. Lett. **78**, 1667 (1997).
[11] S. M. Nie and S. R. Emery, Science **275**, 1102 (1997).
[12] D. J. Bergman and M. I. Stockman, Phys. Rev. Lett. **90**, 027402 (2003).
[13] N. I. Zheludev *et al.*, Nat. Photon. **2**, 351 (2008).
[14] A. Yariv and P. Yeh, *Optical Waves in Crystals* (John Wiley & Sons, NY, 1984).
[15] J. D. Joannopoulos, R. D. Meade, and J. N. Winn, *Photonic Crystals* (Princeton University Press, NJ, 1995).
[16] N. Engheta and P. Pelet, Opt. Lett. **16**, 723 (1991).
[17] M. I. D'yakonov, Sov. Phys. JETP **67**, 714 (1988).
[18] D. B. Walker, E. N. Glytsis, and T. K. Gaylord, J. Opt. Soc. Am. A **15**, 248 (1998).
[19] K. Kato and E. Takaoka, Appl. Opt. **41**, 5040 (2002).
[20] F. Yang and J. R. Sambles, J. Mod. Opt. **40**, 1131 (1993).
[21] I. J. Hodgkinson, S. Kassam, and Q. H. Wu, J. Comput. Phys. **133**, 75 (1997).
[22] O. Takayama *et al.*, Electromagnetics **28**, 126 (2008).
[23] N. S. Averkiev and M. I. D'yakonov, Opt. Spectrosc. **68**, 653 (1990).
[24] J. R. Nelatury, J. A. Polo, Jr., and A. Lakhtakia, J. Opt. Soc. Am. A **24**, 856 (2007).
[25] L. C. Crasovan *et al.*, Opt. Lett. **30**, 3075 (2005).
[26] L. Torner *et al.*, J. Lightwave Technol. **13**, 2027 (1995).
[27] L. Torner *et al.*, Electron. Lett. **29**, 1186 (1993).
[28] S. R. Nelatury, J. A. Polo, Jr., and A. Lakhtakia, Electromagnetics **28**, 162 (2008).
[29] D. Artigas and L. Torner, Phys. Rev. Lett. **94**, 013901 (2005).